Supporting Information to

Small-Angle Scattering and Scale-Dependent Heterogeneity

C.J. Gommes

Contents

I. THE TWO-SCALE MODEL IN FIG. 4 OF THE MAIN TEXT

The theoretical section of the main text is illustrated with a model of porous material comprising two different structural level. The large-scale structure, corresponding to the mesopores, was modelled as a clipped Gaussian random field. The small-scale structure, corresponding to micropores, was modelled as a Boolean model. The two structures are combined into a single model as sketched in Fig. SI-1, i.e. the solid phase of the two-scale structure is the intersection of the solid phases in each substructure. We use the same notation as in the main text, and we refer to the pore space as phase P and the solid phase as S.

Because the two substructures are statistically independent from one another, the two-point probability function of the solid phase in the entire two-scale structure is the following product

$$P_{SS}(r) = P_{SS}^{(1)}(r)P_{SS}^{(2)}(r) \tag{SI-1}$$

where the superscripts 1 and 2 correspond to the small-scale and large-scale structures, respectively.

Evaluating Eq. (SI-1) for $r = 0$, the volume fraction of the solid is obtained as

$$\phi_S = \phi_S^{(1)}\phi_S^{(2)} \tag{SI-2}$$

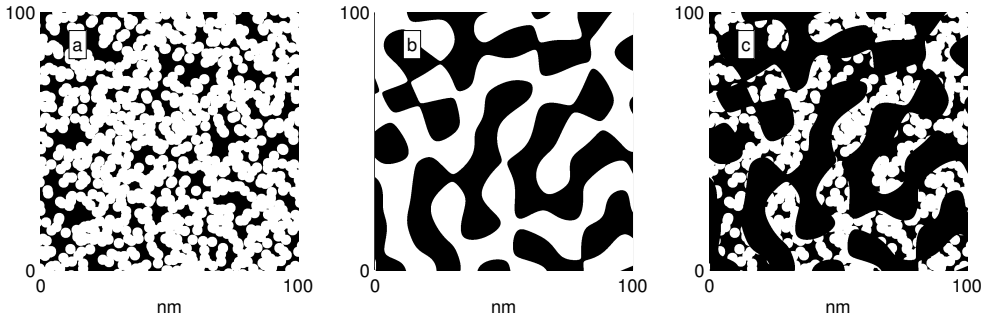

FIG. SI-1: Sketch of the hierarchical model of micro- and meso-porous material. The small-scale structure is modelled a Boolean model (a) and the large-scale structure as a clipped Gaussian random field (b). The overall structure (c) is the intersection of the two levels. The solid phase S is shown in white, and the pore space P is in black.

The surface area of the model is calculated from the derivative of $P_{SS}(r)$ for $r = 0$, which leads to

$$A_{PS} = \phi_S^{(2)} A_{PS}^{(1)} + \phi_S^{(1)} A_{PS}^{(2)} \tag{SI-3}$$

where $A_{PS}^{(i)}$ is the surface area of the i^{th} structure, obtained as

$$\left(\frac{dP_{SS}^{(i)}}{dr} \right)_{r=0} = -\frac{1}{4} A_{PS}^{(i)} \tag{SI-4}$$

where the derivative is estimated for $r = 0$.

In order to calculate the SAXS patterns of the model, we rewrite Eq. (SI-1) in terms of $\chi^{(i)}(r) = P_{SS}^{(i)}(r) - \left[\phi_S^{(i)}\right]^2$ as follows

$$\begin{aligned} \chi(r) &= \chi^{(1)}(r)\chi^{(2)}(r) + \left[\phi_S^{(1)}\right]^2 \chi^{(2)}(r) + \left[\phi_S^{(2)}\right]^2 \chi^{(1)}(r) \\ &\simeq \left[\phi_S^{(1)}\right]^2 \chi^{(2)}(r) + \phi_S^{(2)} \chi^{(1)}(r) \end{aligned} \tag{SI-5}$$

where the second line results from assuming that the characteristic scales of the two structural levels are distinctly different [1]. The SAXS intensity of the model is then calculated by evaluating numerically the Fourier transform of $\chi(r)$.

A. Small-scale structure: Boolean model

In the Boolean model, the solid phase of the material is modelled as the union of spheres with radius R_s, the centres of which are distributed in spaces following a Poisson point process with density θ_s. The volume fraction of the solid phase $\phi_S^{(1)}$ is calculated as [2, 3]

$$\phi_S^{(1)} = 1 - \exp\left(-\theta_s \frac{4\pi R_s^3}{3} \right) \tag{SI-6}$$

and the volume fraction of the pore space is $\phi_P^{(1)} = 1 - \phi_S^{(1)}$. For generating the realisation in the inset of Fig. 4 of the main text, with $\phi_S^{(1)} = 0.7$ and $R_s = 20$ Å, the density θ_s of the underlying Poisson point process was calculated as

$$\theta_s = -\frac{3}{4\pi R_s^3} \ln(1 - \phi_S^{(1)}) \tag{SI-7}$$

The corresponding numerical value is $\theta_s = 0.287\ 10^{-3}$ Å^{-3}.

The two-point probability function of the solid phase is [2, 3]

$$P_{SS}^{(1)}(r) = 2\phi_S^{(1)} - 1 + (1 - \phi_S^{(1)})^2 \exp\left(\theta_s \Omega_s(r)\right) \tag{SI-8}$$

where $\Omega_s(r)$ is the intersection volume of two spheres with radius R_s at a distance r from one another, i.e.

$$\Omega_s(r) = \frac{4\pi R_s^3}{3} \left[\frac{1}{2} \left(\frac{r}{2R_s} \right)^3 - \frac{3}{2} \left(\frac{r}{2R_s} \right) + 1 \right] \tag{SI-9}$$

for $r \leq 2R_s$ and 0 otherwise. From the value of $P_{SS}^{(1)}(r)$ the correlation function is calculated as

$$\chi^{(1)}(r) = (1 - \phi_S^{(1)})^2 \left[\exp\left(\theta_s \Omega_s(r)\right) - 1\right] \tag{SI-10}$$

which is used in Eq. (SI-5) to calculate the SAXS intensity of the model.

From the above formulae, the following expression is obtained for the surface area

$$A_{PS}^{(1)} = -\ln(1 - \phi_S^{(1)})(1 - \phi_S^{(1)}) \frac{3}{R_s} \tag{SI-11}$$

which results from Eq. (SI-4). For R_s =20 Å and $\phi_S^{(1)} = 0.7$, the value is $A_{PS}^{(1)} \simeq 0.0542$ Å^{-1}. This value is equivalent to 542 m^2/cm^3.

B. Large-scale structure: clipped Gaussian random field

The large-scale structure is modelled as a clipped Gaussian random field [4]. In other words, phase S is modelled as the region of space where a given Gaussian random field (GRF) $w(\mathbf{x})$ takes values larger than a given threshold α. The GRF can be seen as resulting from the interference of N random waves, with random wave vectors $\mathbf{q}_i$ and random phase φ_i as

$$w(\mathbf{x}) = \sqrt{\frac{2}{N}} \sum_{i=1}^{N} \cos(\mathbf{q}_i \cdot \mathbf{x} - \varphi_i) \tag{SI-12}$$

If the phases are uniformly distributed in $[0, 2\pi]$, the resulting values of w are Gaussian-distributed with average 0 and the factor $\sqrt{2/N}$ ensures that the variance is equal to 1. The correlation function of the field $g(\mathbf{r})$ is defined as

$$g(\mathbf{r}) = \langle w(\mathbf{x}) w(\mathbf{x}+\mathbf{r}) \rangle \tag{SI-13}$$

and it depends on the statistical distribution of the wave vectors $\mathbf{q}_i$. A convenient form for $g(r)$ is the following [5]

$$g(r) = \frac{1}{\cosh(\kappa r/\lambda)} \frac{\sin(2\pi r/\lambda)}{2\pi r/\lambda} \tag{SI-14}$$

where λ is a characteristic length and κ is a parameter that can be thought of in terms of the disorder of the structure. This form is quadratic at the origin $g(r) \simeq 1 - (r/l)^2$ with

$$\frac{1}{l^2} = \frac{1}{\lambda^2} \left(\frac{2\pi^2}{3} + \frac{\kappa^2}{2} \right) \tag{SI-15}$$

The value of l is needed to calculate the specific surface area of the model, as we show hereunder.

Because the values of the GRF are Gaussian distributed (variance 1, average 0), the solid fraction of the material is

$$\phi_S^{(2)} = \int_{\alpha}^{\infty} \frac{1}{\sqrt{2\pi}} \exp(-t^2/2)\, \mathrm{d}t \tag{SI-16}$$

The two-point probability function $P_{SS}^{(2)}(r)$ is calculated as follows [4]

$$P_{SS}^{(2)}(r) = \phi_S^{(2)} - \frac{1}{2\pi} \int_{\arcsin(g(r))}^{\pi/2} \exp\left(\frac{-\alpha^2}{1+\sin(x)} \right) \mathrm{d}x \tag{SI-17}$$

The specific surface area of the model is obtained from the derivative of $P_{SS}(r)$ in the limit $r \to 0$. This leads to

$$A_{PS}^{(2)} = \frac{2^{3/2}}{\pi} \exp(-\alpha^2/2) \frac{1}{l} \tag{SI-18}$$

The model used in the main text assumes the particular values: $\phi_S^{(2)} = 0.5$ (corresponding to $\alpha = 0$), $\lambda = 200$ Å and $\kappa = 2$. In this case, the two-point function reduces to

$$\chi^{(2)}(r) = \frac{\arcsin(g(r))}{2\pi} \tag{SI-19}$$

and the surface area takes the values $A_{PS}^{(2)} = 0.0132$ Å^{-1}, *i.e.*. 132 m^2/cm^3.

II. SCALE-DEPENDENT HETEROGENEITY WITH A THREE-POINT PROBE

We generalise here the developments of Sec 2.2 of the main text, by considering the scale-dependent heterogeneity defined with the following three-point probe

$$\Pi_r(\mathbf{x}) = \frac{1}{3} \Big[\delta(\mathbf{x} - \mathbf{x}_1) + \delta(\mathbf{x} - \mathbf{x}_2) + \delta(\mathbf{x} - \mathbf{x}_3) \Big] \tag{SI-20}$$

where $\mathbf{x}_1$, $\mathbf{x}_2$ and $\mathbf{x}_3$ are located at the vertices of an equilateral triangle with side r.

In order to calculate the values of the filtered density ρ_π with the three-point probe, as well as their corresponding probabilities, one has to consider three-point probability functions, which generalise the stick-probability function discussed in the main text [6]. In particular, we shall make use of the probability $P_{PPP}(r)$ that the three points of a randomly-oriented equilateral triangle with side r all belong to phase P. This function satisfies $P_{PPP}(0) = \phi_P$ and $P_{PPP}(r) \to \phi_P^3$ for large values of r. For intermediate values of r, $P_{PPP}(r)$ contains higher-order structural information in addition to the volume fraction and standard two-point correlation function.

Besides $P_{PPP}(r)$ one can also define other three-point functions such as $P_{PPS}(r)$, $P_{SSP}(r)$, etc. These three-point functions, however, are not independent from $P_{PPP}(r)$. For example, the probability that two points of the triangle belong to phase P irrespectively of the phase to which the third point belongs is P_{PP}. In other words $P_{PP}(r) = P_{PPP}(r) + P_{PPS}(r)$, which can also be written as

$$P_{PPS}(r) - \phi_P^2\phi_S = \phi_P\phi_S\gamma(r) - \left[P_{PPP}(r) - \phi_P^3\right] \tag{SI-21}$$

Moreover, in the case of isotropic media all the vertices of the equilateral triangle are equivalent so that $P_{PSP}(r) = P_{SPP}(r) = P_{PPS}(r)$. Another relation is obtained observing that the probability that any one point of the triangle belongs to phase P, irrespectively of the phases that the other two points belong to, is nothing but ϕ_P. The latter probability can be decomposed as $P_{PPP} + P_{PPS} + P_{PSP} + P_{PSS}$. This leads to

$$P_{SSP}(r) - \phi_S^2\phi_P = -2\phi_P\phi_S\gamma(r) + \left[P_{PPP}(r) - \phi_P^3\right] \tag{SI-22}$$

Finally, it has to be noted that Eq. (SI-21) would still hold if phases P and S were swapped. Combining this with Eq. (SI-22) leads to

$$P_{SSS}(r) - \phi_S^3 = 3\phi_P\phi_S\gamma(r) - \left[P_{SSS}(r) - \phi_S^3\right] \tag{SI-23}$$

Equations (SI-21), (SI-22) and (SI-23) show that out of the eight possible triangular correlation functions, only one is linearly independent from the two-point correlation function.

Limiting ourselves to the case of isotropic media, the value of ρ_π depends on the three-point probability functions as follows

$$\rho_\pi = \begin{cases} \rho_P & \text{with probability} \quad P_{PPP}(r) \\ (2\rho_P + \rho_S)/3 & \text{with probability} \quad 3 \times P_{PPS}(r) \\ (\rho_P + 2\rho_S)/3 & \text{with probability} \quad 3 \times P_{SSP}(r) \\ \rho_S & \text{with probability} \quad P_{SSS}(r) \end{cases} \tag{SI-24}$$

Using these probabilities, the heterogeneity corresponding to the three-point probe can then be calculated as

$$\begin{aligned} \sigma^2\{\Pi\} &= \rho_P^2 P_{PPP}(r) + \frac{(2\rho_P + \rho_S)^2}{3} P_{PPS}(r) \\ &+ \frac{(\rho_P + 2\rho_S)^2}{3} P_{SSP}(r) + \rho_S^2 P_{SSS}(r) - \langle\rho_\pi\rangle^2 \end{aligned} \tag{SI-25}$$

where the average value is evaluated as $\langle\rho_\pi\rangle = \phi_P\rho_P + \rho_S\phi_S$.

The three-point probability functions individually carry higher-order structural information than the correlation function $\gamma(r)$. However, using the relations from Eqs (SI-21) to (SI-23), one finds the following simple result

$$\sigma^2\{\Pi\} = Q\frac{1 + 2\gamma(r)}{3} \tag{SI-26}$$

which has the same statistical interpretation as Eq. (18) of the main text. Equation (SI-26) depends only on the standard correlation function $\gamma(r)$.

III. PROPERTIES OF THE THREE MAIN PROBES CONSIDERED IN THE MAIN TEXT

A. Spherical probe

The normalised spherical probe of radius R is defined as

$$\Pi_R(\mathbf{y}) = \frac{3}{4\pi R^3}\Theta(R - |\mathbf{y}|) \tag{SI-27}$$

the Fourier transform of which is

$$\hat{\Pi}_R(q) = 3\frac{\sin(qR) - (qR)\cos(qR)}{(qR)^3} \tag{SI-28}$$

The corresponding autocorrelation function $\Omega_R(r)$ is calculated from the intersection volume of spheres at distance r from one another. This leads to

$$\Omega_R(r) = \frac{3}{4\pi R^3}\left\{1 - \frac{3}{2}\left(\frac{r}{2R}\right) + \frac{1}{2}\left(\frac{r}{2R}\right)^3\right\} \tag{SI-29}$$

The following moments of $\Omega_R(r)$ are required for the analysis of the heterogeneity curves $\sigma^2\{\Pi\}$ for small probes

$$\mu_n^\Omega = \int_0^\infty r^n \Omega_R(r) 4\pi r^2 \mathrm{d}r \tag{SI-30}$$

From Eq. (SI-29), one finds

$$\mu_n^\Omega = 12 \times (2a)^n \left(\frac{2}{n+3} - \frac{3}{n+4} + \frac{1}{n+6}\right) \tag{SI-31}$$

This leads to the particular values $\mu_0^\Omega = 1$, $\mu_1^\Omega = (36/35)R$, $\mu_2^\Omega = (6/5)R^2$ and $\mu_3^\Omega = (32/21)R^3$ which are used in the main text. The corresponding values of $\alpha_\pi^{(n)}$ are in Tab. 1 of the main text. The values of $\Omega^{(n)}$ and of $\beta_\pi^{(n)}$ in Tab. 1 are obtained by evaluating the successive derivatives of Eq. (SI-29).

B. Gaussian probe

We define the Gaussian probe as

$$\Pi_a(\mathbf{y}) = \frac{1}{(2\pi)^{3/2}a^3}\exp\left(-\frac{y^2}{2a^2}\right) \tag{SI-32}$$

where a is the standard deviation, which we refer to hereafter as the *size* of the probe. It is to avoid any confusion with the heterogeneity $\sigma^2\{\Pi\}$ that we use the notation a for the standard deviation rather than the usual σ.

The convolution of two Gaussian probes with sizes a and b is itself a Gaussian with size $\sqrt{a^2+b^2}$, i.e.

$$G_a * G_b = G_{\sqrt{a^2+b^2}} \tag{SI-33}$$

Therefore the autocorrelation of a Gaussian probe is

$$\Omega_a(r) = \frac{1}{8\pi^{3/2}a^3}\exp\left(-\frac{r^2}{4a^2}\right) \tag{SI-34}$$

The moments μ_n^Ω are obtained by integrating the latter equation, and taking into account the following general mathematical results

$$\begin{aligned} &\int_0^\infty x^2\exp(-x^2)\mathrm{d}x = \sqrt{\pi}/4 \qquad \int_0^\infty x^3\exp(-x^2)\mathrm{d}x = 1/2 \\ &\int_0^\infty x^4\exp(-x^2)\mathrm{d}x = 3\sqrt{\pi}/8 \qquad \int_0^\infty x^5\exp(-x^2)\mathrm{d}x = 1 \end{aligned} \tag{SI-35}$$

The result is

$$\begin{aligned} &\mu_0^\Omega = 1 \qquad \mu_1^\Omega = 4a/\sqrt{\pi} \\ &\mu_2^\Omega = 6a^2 \quad \mu_3^\Omega = 32a^3/\sqrt{\pi} \end{aligned} \tag{SI-36}$$

The values of $\alpha_\pi^{(n)}$ gathered in Tab. 1 of the main text are obtained from the latter values of μ_n^Ω. The values of $\Omega^{(n)}$ and of $\beta_\pi^{(n)}$ in Tab. 1 are obtained by evaluating the successive derivatives of Eq. (SI-34).

C. q-Spherical probe

We define the q-sphere $J_\nu(\mathbf{y})$ as the probe, the Fourier transform of which is a sphere of radius ν in reciprocal space. The Fourier transform of this probe is

$$\hat{\Pi}_\nu(q) = \Theta\left(\nu - |\mathbf{q}|\right) \tag{SI-37}$$

The parameter ν can be thought of as a cutoff frequency, which is related to a characteristic size L of the probe in real-space via the inverse relation $L \simeq 1/\nu$. The real-space expression is obtained by a Fourier transform, which leads to

$$\Pi_\nu(\mathbf{y}) = \frac{\nu^3}{6\pi^2}\frac{3[\sin(\nu|\mathbf{y}|) - (\nu|\mathbf{y}|)\cos(\nu|\mathbf{y}|)]}{(\nu|\mathbf{y}|)^3} \tag{SI-38}$$

This probe has the intriguing property of being stable by convolution. For example, the autocorrelation of Π_ν is given by the same expression as Π_ν itself, namely

$$\Omega_J(r) = \frac{\nu^3}{6\pi^2}\frac{3[\sin(\nu r) - (\nu r)\cos(\nu r)]}{(\nu r)^3} \tag{SI-39}$$

This results from the fact that $\hat{\Pi}_\nu$, the Fourier transform of Π_ν, is a binary function that can only take the values 0 or 1. The Fourier transform is therefore left unchanged if it is raised to the power two: $\hat{\Pi}_\nu = \hat{\Pi}_\nu^2$. In real-space, this converts to a stability with respect to the autocorrelation.

It is difficult to estimate the moments μ_n^Ω by a direct evaluation, because the integrals of the type

$$\frac{\nu^3}{6\pi^2}\int_0^\infty r^n \frac{3[\sin(\nu r) - (\nu r)\cos(\nu r)]}{(\nu r)^3}\, 4\pi r^2\, \mathrm{d}r \tag{SI-40}$$

do not converge for $n \geq 1$. We therefore use a different approach.

Quite generally, the form factor $P_\pi(q)$ of any probe is the Fourier transform of $\Omega_\pi(r)$, namely

$$P_\pi(q) = \int_0^\infty \frac{\sin(qr)}{qr}\Omega_\pi(r)4\pi r^2 \mathrm{d}r \tag{SI-41}$$

Developing $\sin(qr)/(qr)$ as a Taylor series

$$\frac{\sin(qr)}{qr} = 1 - \frac{1}{3!}(qr)^2 + \frac{1}{5!}(qr)^4 - \frac{1}{7!}(qr)^6 + \dots \tag{SI-42}$$

shows that all the moments of even order are proportional to the equivalent derivative of P_π for $q = 0$. The actual relation is

$$\left(\frac{d^{2n}P_\pi}{dq^{2n}}\right)_{q=0} = \frac{(-1)^n}{2n+1}\mu_{2n}^\Omega \tag{SI-43}$$

This equation is quite general. In the particular case of the q-sphere, it shows that all moments of even order are equal to zeros because $P_\pi(q)$ is a constant close to $q = 0$. In particular, we have $\mu_2^\Omega = 0$.

The moments of odd order are obtained also in an indirect way, from the following general asymptotic relation for the SAXS intensity

$$I(q) = 8\pi Q\left(\frac{-\gamma^{(1)}}{q^4} + \frac{2\gamma^{(3)}}{q^6} + \frac{-3\gamma^{(5)}}{q^8} + \dots\right) \tag{SI-44}$$

where γ^n are the n^{th} derivatives of the correlation function $\gamma(r)$ for $r = 0$. Equation (SI-44) is the classical Kirste-Porod expression [7], which can be obtained from the direct expression of $I(q)$ as the Fourier transform of $\gamma(r)$ via integration by parts. When this asymptotic expression is used in the expression of $\sigma^2\{\Pi\}$ in reciprocal space, one finds

$$\sigma^2\{\Pi\} \;=\; \text{constant} + \frac{1}{(2\pi)^3}\int^\nu 8\pi Q\left(\frac{-\gamma^{(1)}}{q^4} + \frac{2\gamma^{(3)}}{q^6} + \frac{-3\gamma^{(5)}}{q^8} + \dots\right)\, 4\pi q^2 \mathrm{d}q$$

$$= \text{ constant} + Q\left[\frac{4\gamma^{(1)}}{\pi\nu} - \frac{8\gamma^{(3)}}{3\pi\nu^3} + \frac{12\gamma^{(5)}}{5\pi\nu^5} + \dots\right] \tag{SI-45}$$

Because of the unknown additive constant, the value of the lower integration bound does not matter. A direct comparison with Eq. (21) of the main text leads to

$$\mu_1^{\Omega} = \frac{4}{\pi\nu} \quad \text{and} \quad \mu_3^{\Omega} = -\frac{16}{\pi\nu^3} \tag{SI-46}$$

and the corresponding values of $\alpha_\pi^{(n)}$ are reported in Tab. 1 of the main text. The values of $\Omega^{(n)}$ and of $\beta_\pi^{(n)}$ in Tab. 1 are obtained by evaluating the successive derivatives of Eq. (SI-39).

---

[1] C. J. Gommes, G. Prieto, and P. E. De Jongh, J. Phys. Chem C **120**, 1400 (2016).
[2] J. Serra, *Image Analysis and Mathematical Morphology*, Vol. 1 (Academic Press, London, 1982).
[3] W. Gille, Computers and Structures **89**, 2309 (2011).
[4] P. Levitz, Advances in Colloid and Interface Science **76-77**, 71 (1998).
[5] C. J. Gommes and A. P. Roberts, Phys. Rev. E **77**, 041409 (2008).
[6] S. Torquato, *Random Heterogeneous Materials* (Springer, New York, 2000).
[7] O. Glatter and O. Kratky, *Small Angle X-ray Scattering* (Academic Press, New York, 1982).